

# Realistic simulation of flutter flight tests

**P. Vacher, A. Bucharles**

ONERA, Department of Systems Control and Flight Dynamics,  
2, av. Edouard Belin, B.P. 4025, 31500 TOULOUSE, FRANCE  
e-mail: [Pierre.Vacher@onera.fr](mailto:Pierre.Vacher@onera.fr), [Alain.Bucharles@onera.fr](mailto:Alain.Bucharles@onera.fr)

## Abstract

In the framework of the FLITE 2 project, identification algorithms were developed in order to monitor the evolution of the aeroelastic modes of an aircraft during flutter flight tests. Simulated data were required to evaluate and compare the algorithms and also to test their ability to detect the onset of flutter.

This paper describes how this simulation was carried out. It presents the model used to simulate the aeroelastic behaviour of the aircraft. A realistic simulation of the in-flight disturbances was also needed to evaluate the identification algorithms in conditions similar to operational conditions. The modeling and simulation of these perturbations constitute another essential feature of this paper. The last point of the article is devoted to the design of appropriate excitation signals.

## 1 Introduction

Flutter tests represent a major stage in the certification procedure of a new aircraft. The objectives are to demonstrate the absence of instability throughout the flight envelop and to check the compliance of the aircraft actual behaviour with predicted aeroelastic models.

For the time being, AIRBUS flutter tests consist in applying calibrated excitations to the aircraft structure for a set of predefined flight conditions where the speed and the altitude of the aircraft are maintained constant.

In the framework of the TRAMPOLINE working group of the FLITE 2 project, a new scenario was devised in collaboration with AIRBUS in order to reduce the duration of the flutter tests and consequently their cost. The objective for the academic partners was to develop identification algorithms adapted to this new testing procedure. Simulated data were therefore required to evaluate and compare these algorithms.

This paper describes how the simulation was carried out. It is organized as follows. The first section is devoted to the context of the simulation, i.e the new scenario and the attendant requirements for the simulation. The global organization of the simulation is presented in the second section. The following three sections are dedicated to the description of the most important aspects of the simulation: the aeroelastic model, the simulation of in-flight perturbations, the simulation of calibrated flutter tests.

## 2 Context of the simulation

### 2.1 A new scenario for flutter testing

Current flight tests are composed of several series of tests performed at *stabilized flight points*, i.e. at constant Mach number  $\mathcal{M}$  and conventional speed  $V_c$  in order to explore the whole flight envelop of an aircraft. As illustrated in the upper part of Figure 1, each series is performed at a constant Mach number  $\mathcal{M}$  with increasing values of  $V_c$ . The current testing protocol is based on a few sine-sweep tests that are interspersed

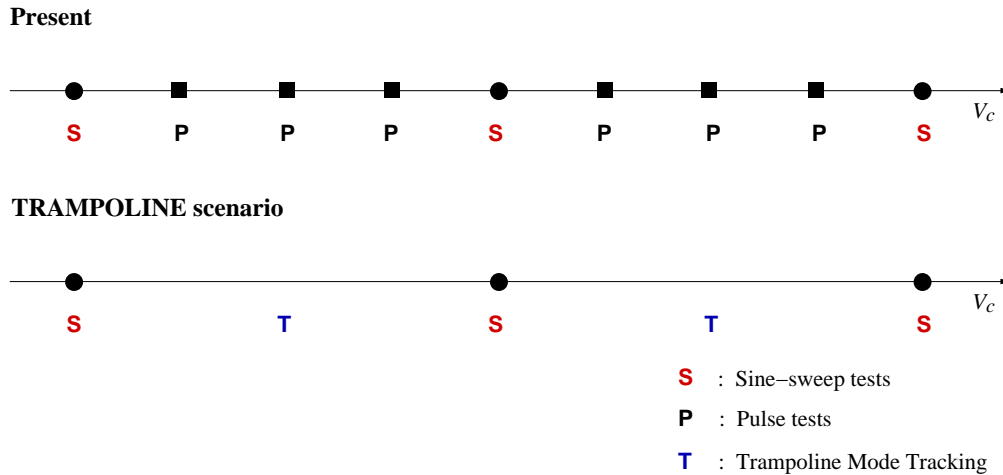


Figure 1: TRAMPOLINE scenario for flutter surveillance

with pulse tests performed at intermediate speeds. Though these latter tests provide less accurate mode estimates, they are used because of their much shorter duration.

According to AIRBUS, as flutter is a critical and hazardous phenomenon, flutter flight tests will always include calibrated excitation tests performed at a few stabilized flight points. The idea of the TRAMPOLINE scenario (**TR**acking **M**odal **P**arameters **O**n**L**INE), illustrated by the lower part of figure 1, is to replace the intermediate pulse tests by a *uniformly accelerated* phase where the evolution of the modal parameters would be monitored continuously. This accelerated phase is called the *transition phase* between two stabilized points. This procedure would lead to a substantial reduction of the overall duration of the flutter tests.

## 2.2 Objectives of the TRAMPOLINE working group

So the objective for the academic partners was to devise identification algorithms that could perform a *continuous tracking of the aeroelastic modes* during the transition phases.

Two categories of methods were investigated:

- *output-only methods* which do not require any experimental excitation.
- *input-output methods* designed to process flight tests with exogenous excitations.

In the first case, the aircraft structure is only excited by operational disturbances. Most of the methods studied in the FLITE 1 project were output-only methods. In the second case, additional well-defined excitation signals are applied to the aircraft control surfaces.

Flight tests are actually affected by two types of operational perturbations. The measurements are corrupted by a permanent *background noise* which is mainly due to the aerodynamic flow around the aircraft. The other type of perturbation is the *air turbulence* which is produced by disturbances in the atmosphere the aircraft is flying through. These disturbances occur *sporadically* as wind gusts and areas of air agitation are encountered by the aircraft. Studies performed in the framework of the FLITE 1 project showed that turbulence is a very efficient means to excite the aircraft structure.

To evaluate the two categories of identification methods on the TRAMPOLINE scenario, three flight conditions were retained for the transition phases:

- *quiet operational conditions*, i.e. background noise only
- *turbulent operational conditions* : background noise and turbulence gusts
- *experimental conditions* : background noise and calibrated excitations

Though turbulence is not an acceptable way to test an aircraft since the occurrence of gusts is quite unpredictable, it was introduced in the scenario as a logical continuation of the FLITE 1 project where this case

was studied. But one of the main goals of the FLITE 2 project was to investigate whether the aircraft modes can be identified in quiet operational conditions which is the most common case. For the experimental conditions, the efficiency of various excitation signals was addressed by the selection of two signals described in section 6.

The global objective of the TRAMPOLINE working group is then to inquire about the feasibility to track the aeroelastic modes during the transition phases in the three aforementioned conditions. Stated differently, the goal is to evaluate the quality of the identified modes for the three selected flight conditions and to determine if this level of quality is sufficient for flutter surveillance and industrial applications.

## 2.3 Requirements for the simulation

Simulated data are the only way to assess the TRAMPOLINE scenario because no flight data are currently available for this new testing procedure. As compared to real flight tests, a simulation also allows a more precise analysis since the true modal parameters are known. The various flight conditions mentioned above can be easily generated and also fairly compared by using the same background noise sequence. Moreover the ability of the algorithms to detect the occurrence of flutter can safely be tested by performing an appropriate simulation of flutter onset. It is however essential that the simulated data realistically replicate real flight test data.

As compared to conventional simulations, the first innovative feature of this study concerns the simulation of the aeroelastic behaviour of an aircraft during an *accelerated flight phase*. The simulation should also simulate various phenomenons : the background noise, the aircraft response to turbulence gusts and to calibrated excitations. The first two ones are random phenomenons. Stochastic characterizations are therefore needed in order to accurately mimic real measurements. These characterizations were determined by the analysis of flight test data as described in section 5.

In summary, the innovative requirements of the simulation presented in this paper are:

- the simulation of an aeroelastic behaviour during an *accelerated flight phase*
- the simulation of random *in-flight perturbations* : background noise, aircraft response to turbulence

## 3 General organization of the simulation

The development of the simulation was greatly oriented by the structure of the aeroelastic model that was provided by AIRBUS. The model used in the FLITE 2 project does not actually correspond to a real aircraft: the modal parameters were modified both for industrial confidentiality reasons and for simulating a flutter case.

As shown in figure 2, this aeroelastic model constitutes the central piece of the simulation tool. This is a linear model derived for a given Mach number  $\mathcal{M}$  from a finite element modeling of the aircraft. It is parametrized by the conventional speed  $V_c$  and includes two types of input:

- the deflections of the control surfaces
- the components of the turbulence speeds

The truthfulness of this model was assumed in the simulation because it was not possible to check its representativeness as it does not correspond to a real aircraft.

As depicted in figure 2 and detailed in the forthcoming sections, other elements must be introduced and adequately tuned for a precise simulation:

- the dynamics of the actuators must be taken into account.
- spectra of the spatial distribution of the turbulence are needed for generating consistent wind components.

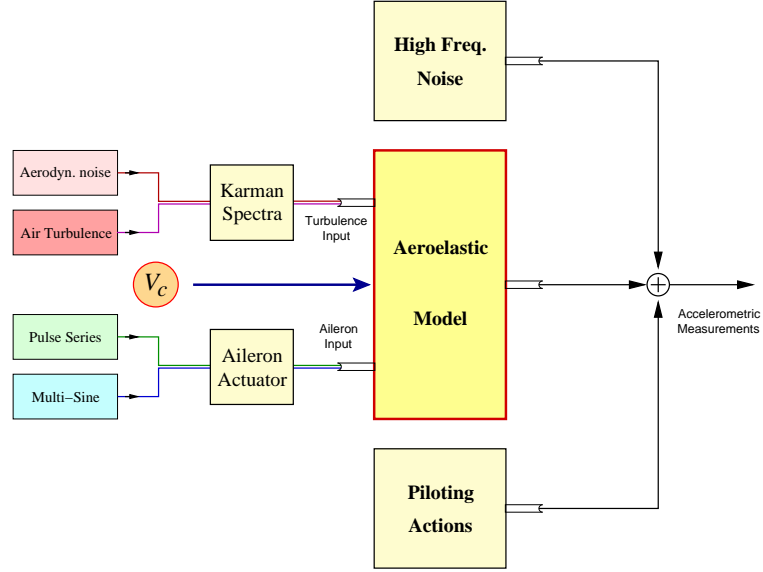


Figure 2: General organization of the simulation

It will also be shown later that the background noise is actually composed of three contributions:

- a high frequency noise.
- a low-level turbulence component
- the aircraft response to piloting actions

## 4 The aeroelastic model

The first subsection concerns the physical definition of the aeroelastic model. The second one describes the associated state-space form which is more appropriate to modal analysis and numerical integration. The third subsection presents the integration method that was adopted to efficiently simulate this time-variant system.

### 4.1 The model definition

The aeroelastic equations define the time evolution of the vector  $\mathbf{q}(t)$  of the structure generalized displacements by the second-order differential equation 1. The left-hand side of this equation concerns the structural efforts while the right-hand side is the sum of various external forces. The vector of the measurements  $Z(t)$  depends linearly on  $\mathbf{q}(t)$  and its first and second derivatives according to equation 2.

$$M \ddot{\mathbf{q}}(t) + (A + G) \dot{\mathbf{q}}(t) + K \mathbf{q}(t) = F_a(t) + F_c(t) + F_t(t) \quad (1)$$

$$Z(t) = \Phi \begin{bmatrix} \mathbf{q}(t) \\ \dot{\mathbf{q}}(t) \\ \ddot{\mathbf{q}}(t) \end{bmatrix} \quad (2)$$

- $\mathbf{q}(t)$  : Vector of the generalized displacements
- $M, A, K$  : Structural mass, damping and stiffness.
- $G$  : Gyroscopic terms due to the engines
- $F_a(t)$  : Unsteady aerodynamic forces
- $F_c(t)$  : Control surface forces function of the deflections  $\delta(t)$
- $F_t(t)$  : Turbulence forces function of the wind speeds  $W(t)$

For a given Mach number  $\mathcal{M}$ , the external forces are interpolated in the frequency domain using the Roger rational approximation [1]:

$$F_a(\bar{s}) = p_{\text{dyn}} \left( P_{a,0} + P_{a,1} \bar{s} + P_{a,2} \bar{s}^2 + \sum_{i=1}^5 R_{a,i} \frac{\bar{s}}{\bar{s} + \gamma_{a,i}} \right) \mathbf{q}(s) \quad (3)$$

$$F_c(\bar{s}) = p_{\text{dyn}} \left( P_{c,0} + P_{c,1} \bar{s} + P_{c,2} \bar{s}^2 + \sum_{i=1}^5 R_{c,i} \frac{\bar{s}}{\bar{s} + \gamma_{c,i}} \right) \boldsymbol{\delta}(s) \quad (4)$$

$$F_t(\bar{s}) = p_{\text{dyn}} \left( P_{t,0} + P_{t,1} \bar{s} + \sum_{i=1}^{12} R_{t,i} \frac{\bar{s}}{\bar{s} + \gamma_{t,i}} \right) \frac{W(s)}{V_{\text{tas}}} \quad (5)$$

where  $\bar{s} = s/V_{\text{tas}}$  is the reduced Laplace variable while  $s$  is the conventional Laplace variable. In these equations,  $p_{\text{dyn}}$  denotes the dynamic pressure and  $V_{\text{tas}}$  the true airspeed. The coefficients  $P_{a,i}$ ,  $P_{c,i}$ ,  $P_{t,i}$  and  $R_{a,i}$ ,  $R_{c,i}$ ,  $R_{t,i}$  are computed by the Roger method for a given Mach number  $\mathcal{M}$ . The modes  $\gamma_{a,i}$ ,  $\gamma_{c,i}$ ,  $\gamma_{t,i}$  correspond to *aerodynamic delays*.

## 4.2 The state-space form

For given Mach number  $\mathcal{M}$  and conventional speed  $V_c$ , one can compute the quantities  $p_{\text{dyn}}$ ,  $V_{\text{tas}}$  needed in equations 3–5. Thus, for a fixed  $\mathcal{M}$ , equations 1 and 2 can be recast into a conventional state-space representation where the state matrices are parametrized by  $V_c$ :

$$\dot{X} = A(V_c) X + B_c(V_c) \boldsymbol{\delta} + B_t(V_c) W \quad (6)$$

$$Z = C(V_c) X + D_c(V_c) \boldsymbol{\delta} + D_t(V_c) W \quad (7)$$

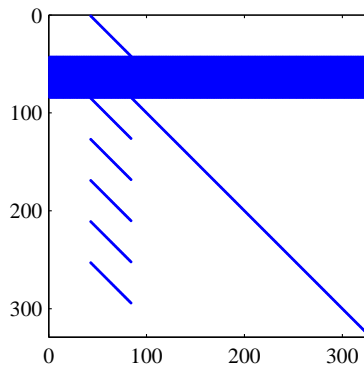


Figure 3: Structure of the state matrix  $A$

In the model of the TRAMPOLINE scenario, the size of the state is equal to 328. The state matrix  $A$  has a specific structure depicted by the sparsity pattern in figure 3. It includes 42 structural modes and 244 delay modes. The input vector  $\boldsymbol{\delta}(t)$  is composed of the deflection of left and right ailerons and their first and second

derivatives and of the wind components<sup>1</sup> and their first derivative. Thirteen measurements were simulated for the TRAMPOLINE scenario.

From the state equation 6, the variation of the modal parameters with respect to  $V_c$  can be computed. For the model used for the TRAMPOLINE simulation, these quantities are depicted in figure 5 which only include the modes below 6 Hz between 330 kts and 360 kts. We can notice that some modes have quite close frequencies and that the mode number 4 evolves towards instability.

### 4.3 Numerical integration

The initial objective for integrating the model described by equations 6 and 7 was to use the same sampling rate as the one used for flight tests, i.e. 128 Hz.  $V_c$  can then be considered constant between two sampling time and a straightforward way to integrate equation 6 is to compute the associated discrete form. However this approach proved to be quite time consuming as it requires the computation of the exponentials of a large matrix at each sampling time.

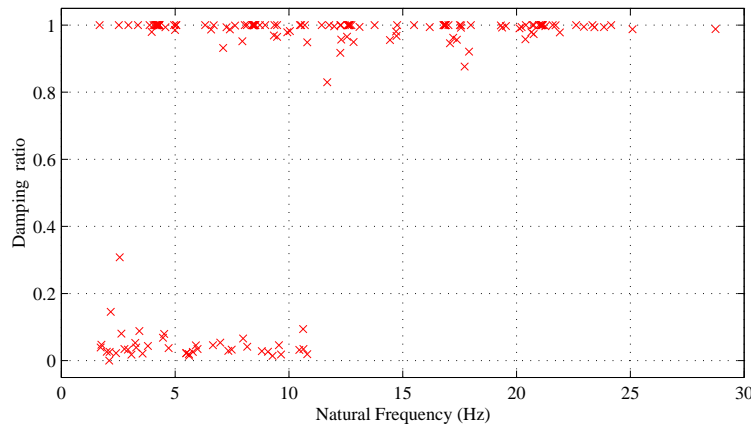


Figure 4: Modes of an aeroelastic model

In order to alleviate the computational load, other integration methods that do not rely on matrix exponentials have to be considered such as the Runge-Kutta methods [2, 3, 4]. However, the order of the integration method must be chosen appropriately so to achieve a compromise between the computation load and the mode distortion induced by the method. It is actually essential that the alteration of the modal parameters be negligible since they are the quantities to be identified.

At the flutter speed, the system modes are depicted in figure 4. One can notice two groups of modes:

- 42 lightly damped modes which correspond to the physical aeroelastic modes.
- 86 aperiodic modes and 79 modes highly damped modes which are related to aerodynamic delays.

According to the study presented in [5], a third order Runge-Kutta would be sufficient for the integration the sole aeroelastic modes. But, for the aerodynamic delays modes, a fifth order method is not sufficient. The accurate simulation of the system thus requires to increase the sampling frequency. If the sampling rate is doubled to 256 Hz, the fourth order procedure is then suitable for the integration of the model.

A 256 Hz sampling rate and a fourth order Runge-Kutta method were then used to integrate the aeroelastic model. In order to speed up the computation, the sparsity of the state matrices as depicted in figure 3 for the matrix  $A$  was taken into account in the implementation of the simulation. The simulation of a 5 minute transition phase requires about 13 min on a 1 GHz Sun workstation. In a subsequent step, the simulated measurements are decimated at the 32 Hz rate required for the TRAMPOLINE tracking application.

<sup>1</sup>For some unknown reason, the turbulence component along the  $z$ -axis was missing in Airbus model.

Transition phase – Model Youpi –  $V_c = 330 \rightarrow 360$  kts

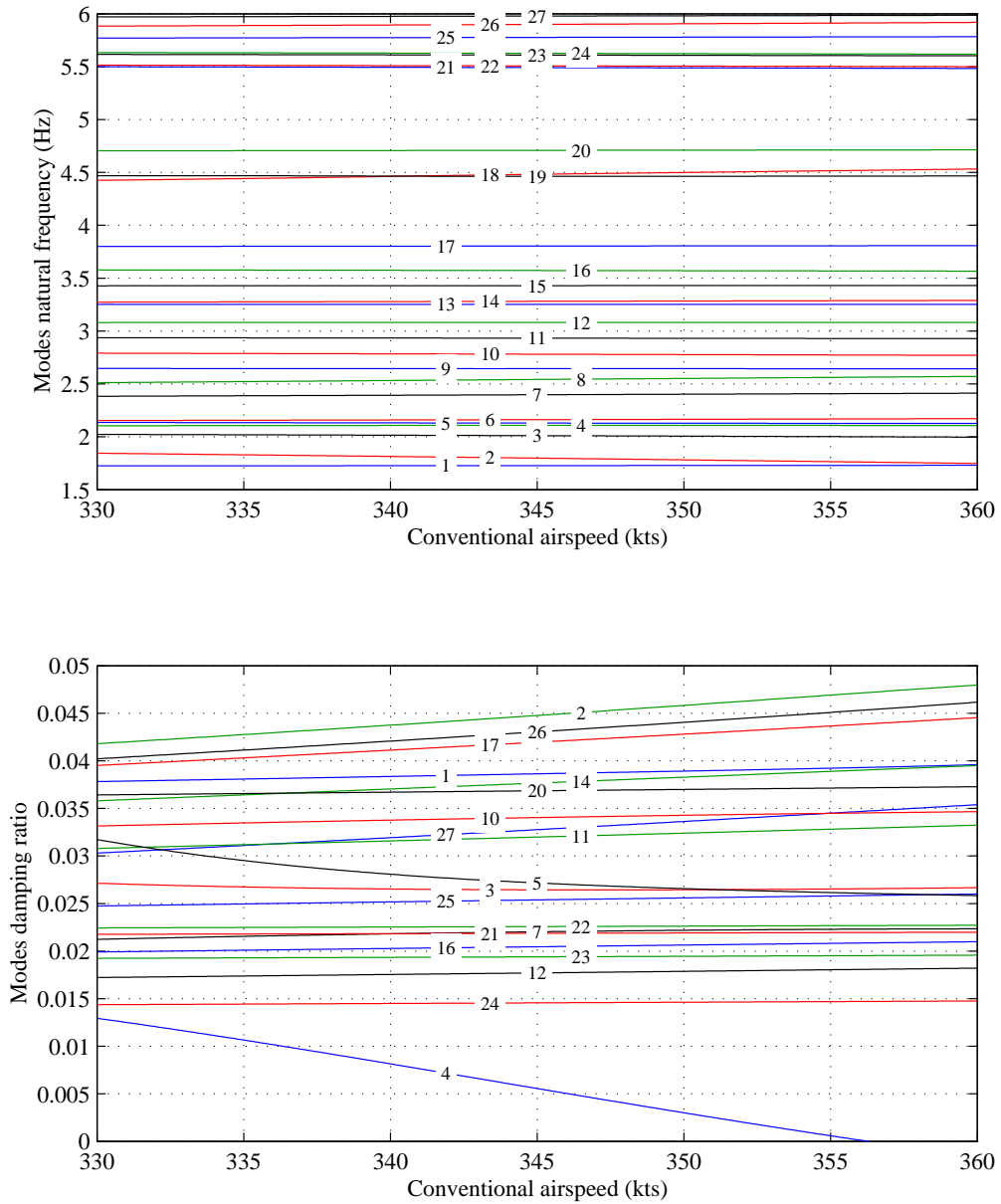


Figure 5: Evolution of the modal parameters during the transition phase

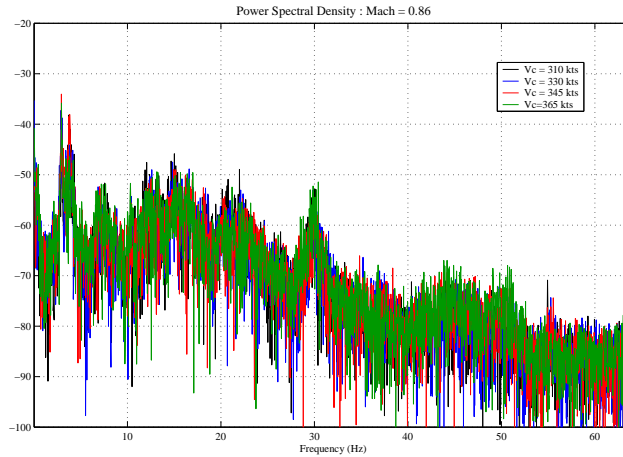


Figure 6: Variation of noise spectra with  $V_c$

## 5 In-flight perturbations

As stated in section 2.2, one can distinguish two types of perturbations : the air turbulence and the background noise. Turbulence is a well-studied phenomenon in aeronautics. All the elements necessary for simulating the response of the aircraft to turbulence gusts are available : the aeroelastic model described in section 4 incorporates an input for the wind components; in the literature [6, 7, 8] one can also find analytical expressions of the turbulence spatial spectra. Finally, the intensity of these spectra can be tuned with real flight data.

On the contrary, little information is available for the background noise. Anyhow this aspect is quite important for the simulation since this noise *permanently* affects the measurements. It is therefore essential in a first step to characterize this noise.

### 5.1 Characterization of the background noise

Concerning this noise, a few questions can be asked:

- Does it share any similarity with turbulence ?
- Can it provide any information about the aeroelastic modes ?
- How does it evolve with the conventional speed  $V_c$  ?

The second question is of major importance for output-only identification. If this background noise does not include any information on the aeroelastic behaviour of the aircraft, it is hopeless to try to identify the modes in quiet operational conditions. The answer to the last question is necessary for the simulation of the transition phase where  $V_c$  increases.

#### 5.1.1 Dependency of the background noise on $V_c$

Several tests performed at the same Mach number with different values of  $V_c$  were analyzed. Power spectral densities<sup>2</sup> PSDs were computed from time intervals where no excitation was applied. Figure 6 give a typical illustration of the PSDs of a measurement for four values of  $V_c$ . We can notice that these densities are nearly identical. The constancy of the PSDs with  $V_c$  is also confirmed by the evolution standard deviations with  $V_c$ . Except for a few measurements, no real tendency can be observed.

The shape of these PSDs also reveals resonances indicating that this signal includes information about structural modes.

<sup>2</sup>The periodogram [9] method was used since those time intervals are generally short.



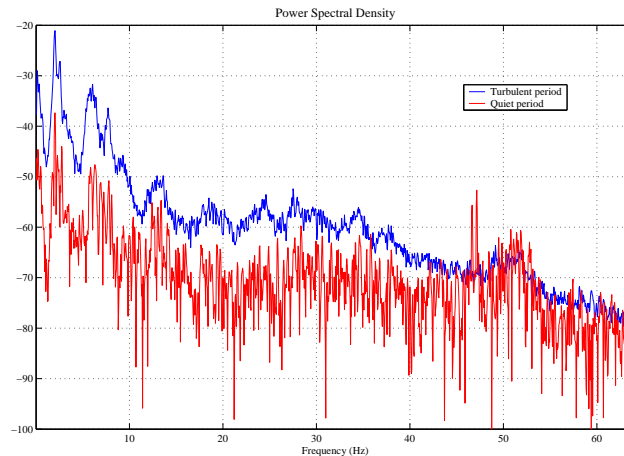


Figure 7: Comparison between quiet and turbulent flight conditions

### 5.1.2 Comparison with turbulence

The comparison of PSDs between a quiet flight period and a turbulent one<sup>3</sup> is illustrated in figure 7. It shows that the general shape of the two PSDs is very similar. They have comparable resonances. The only different is the level which is of course higher for the turbulent period up to 45 Hz approximately.

From these observations, one can infer that two main conclusions. First the background noise is similar to turbulence but with a lower intensity. So an approach similar to turbulence can be used to simulate it though, as described hereafter, other contributions should also be considered. The second essential point is that, similarly to turbulence, the background noise incorporates information about the response of the aeroelastic modes but at a smaller level.

## 5.2 Simulation of the perturbations

If the major part of the background noise can be considered as a low intensity turbulence, one must also take into account other aspects to simulate this noise. As illustrated by figure 8, three contributions were considered. Each of them concerns a specific frequency band:

- the response of the aircraft to piloting actions at low frequencies
- the response of the aircraft to a permanent low-level turbulence at intermediate frequencies.  
This contribution is called the “aeroelastic noise”
- high-frequency perturbations

These latter are intended to encompass all the disturbing phenomenons that occur above the frequency band of interest for the TRAMPOLINE application. The following paragraphs describe how these three components were simulated. The “aeroelastic noise” description covers both the contribution to the background noise and the aircraft response to turbulence.

### 5.2.1 Piloting actions

The correct way to simulate the effect of piloting inputs on the accelerometric measurements would be to consider a flight dynamics model of the aircraft and to simulate the pilot’s action on the stick or the commands generated by the flight control system. A simpler approach was adopted in order to replicate two aspects of this contribution : its spectral density and its correlation between the measurements. The following procedure was used:

<sup>3</sup>As the turbulent period was longer, the Welch procedure [10] was used to smooth the PSDs.

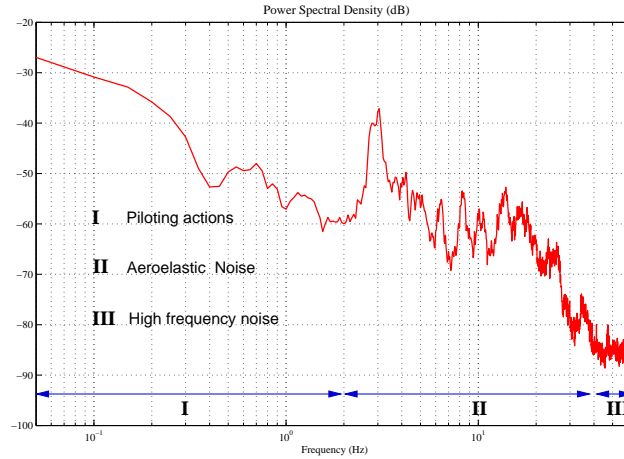


Figure 8: The three frequency zones for the simulation of the background noise

- Random Markov processes meant to mimic the pilot actions in the Cartesian directions were generated. The order and the cut-off frequencies of these processes were estimated from real flight data.
- The level of the contribution of these processes on each sensor was determined by the analysis of flight data.

### 5.2.2 Aeroelastic noise

For the simulation of the aircraft response to turbulence, the turbulence inputs of the aeroelastic model were used presuming that they produce a realistic behaviour of the aircraft in turbulent conditions.

The  $W_x$  and  $W_y$  components of turbulence were generated according to the von Karman spectra [6, 7, 8] given by

$$\Phi_{W_x}(\omega) = \frac{\sigma_x^2}{\pi} \frac{2 L_x}{V} \frac{1}{(1 + (a L_x \frac{\omega}{V})^2)^{5/6}} \quad (8)$$

$$\Phi_{W_y}(\omega) = \frac{\sigma_y^2}{\pi} \frac{L_y}{V} \frac{1 + \frac{8}{3} (a L_y \frac{\omega}{V})^2}{(1 + (a L_y \frac{\omega}{V})^2)^{11/6}} \quad (9)$$

The quantities  $L_x$  and  $L_y$  are the spatial scales<sup>4</sup> of turbulence and  $a$  is a constant defined such that the integrals of the above expressions w.r.t  $\omega$  are equal to the variances  $\sigma_x^2$  and  $\sigma_y^2$ .

The standard deviations  $\sigma_x$  and  $\sigma_y$  were estimated from real flight data. For the background noise, satisfactory results were obtained. However, for turbulent conditions, difficulties were encountered in finding values for which the levels of the fluctuations on the simulated measurements were in accordance with real flight data. This might be due to some lack of representativity of this modified aeroelastic model or to the fact that the  $W_z$  is missing in the AIRBUS model. A compromise was achieved by adopting, for  $\sigma_x$  and  $\sigma_y$ , values four times greater than the ones used for the background noise.

### 5.2.3 High frequency noise

This noise is supposed to simulate the various disturbances in the high frequencies, i.e. above the frequency band specified for the TRAMPOLINE problem. A simple Gaussian noise sequence was used for each measurement with a standard deviation determined from real data.

<sup>4</sup>The values recommended in the references were used:  $L_x = L_y = 2500$  ft.

## 6 Calibrated tests

For simulating the aircraft response to calibrated excitation applied to the control surfaces, we first need a model of the actuators. Then, appropriate excitation signals must be defined.

### 6.1 Actuator dynamic model

The model proposed by AIRBUS is a second-order linear model. But, from practical experience, we know that the actuator dynamics is non-linear especially for pulse tests. As depicted in figure 9, the actual deflection of an aileron is highly dependent on the sign and on the amplitude of the pulse input signal. As it might have a significant impact on the results of identification methods, an accurate simulation of this behaviour is desirable. Anyhow, it would require a much more complex modeling which would take into account various aspects such as the actuator torque limitation, the aerodynamic hinge moment on the control surface, the control law of the actuator.

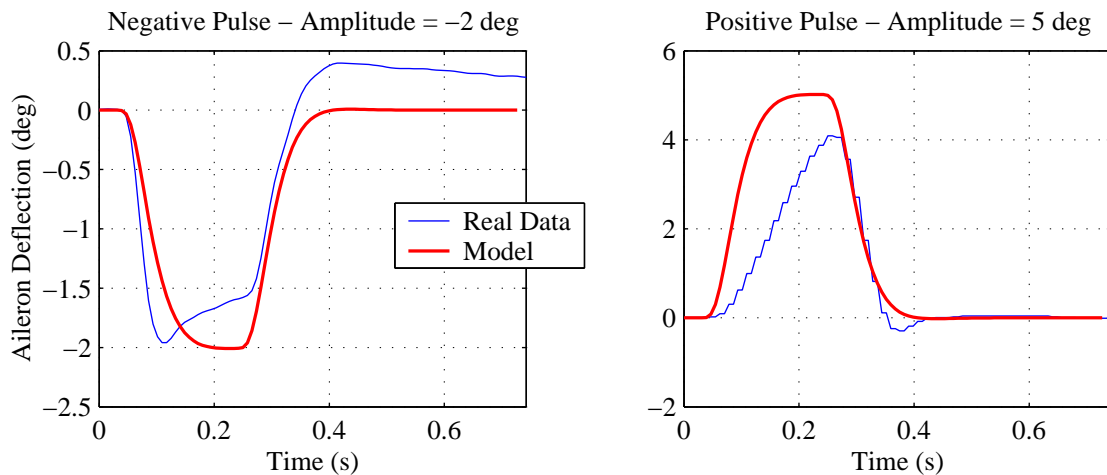


Figure 9: Actual response of the aileron actuator to a pulse excitation

It was then decided to keep the linear model though the comparisons with true deflections show that the model response is most of the times “optimistic”.

### 6.2 Selection of the excitation signals

This selection was guided by the same approach used nowadays for the flight tests which are based on two types of excitations: sine-sweep and pulses. The sine-sweep signal covers exactly the frequency range of interest and allows a precise identification of the modes of the aircraft. On the other hand, pulse tests are much shorter and their goal is more to assess the global stability of the aircraft than the accurate identification of the modes.

Experience also shows that identification methods can behave quite differently depending whether the excitation signal is persistent or intermittent. So the other objective for this selection was to evaluate the behaviour of the identification algorithms for these two types of excitation.

This led us to consider two excitations for the transition phases of the TRAMPOLINE scenario:

- a pulse series applied on a single aileron
- two multi-sine applied symmetrically and anti-symmetrically on both ailerons

### 6.2.1 Pulse series

For simplicity purposes, this excitation is applied on a single aileron so as to excite simultaneously symmetrical and anti-symmetrical modes. During the transition phase, one pulse is issued every 20 s.

### 6.2.2 Multi-sine excitation

Sine-sweeps could also have been used during the transition phase. Anyhow the policy at AIRBUS is to reduce the number of sweep tests because they are associated with the notion of lengthy and costly tests. In order to gain the acceptance of the test teams, multi-sine signals are proposed.

Similarly to sine-sweeps, they concentrate the excitation energy on the sole frequency band of interest. In the time domain, they also present the appearance of random signals which could be assimilated to a “calibrated turbulence”.

The basic period of the multi-sine was chosen equal to the period of the pulse series: 20 s. The multi-sine signals were computed by the clipping algorithm [11] over the 0.5–6 Hz frequency band specified for TRAMPOLINE.

## 7 Results and conclusion

The comparison between simulated and real measurements is only possible for tests performed at a constant speed. This is illustrated for a few measurements in figure 10. Of course, as the modes of the real and simulated modal are different, their responses are also different. But the global visual aspect of the aircraft response and of the noise on the measurements is quite similar.

Figure 11 depicts the simulation for an accelerated phase for the case of quiet operational conditions (background noise). The evolution of the associated modal parameters are plotted above in figure 5. The time when the model becomes unstable is indicated by a red dashed line. Even without any external excitation, this instability is quite evident of some measurements. So, even for this case without any external excitation, the flutter onset should be detectable by the identification algorithms.

The previous examples demonstrate the realism of the simulation. One of the main findings of this study is the characterization of the background noise which showed that this noise includes contributions from the aeroelastic modes. This opens the possibility to identify the modes in standard operational conditions.

Anyhow, the simulation could be improved on several points. First the representativeness of the turbulent model should be checked and improved with an aeroelastic model corresponding to a real aircraft and with a full turbulence input vector.

Secondly, this simulation is not generic but very specific of an aircraft and of the flight conditions. That is to say that real flight data are needed in the same flying conditions to tune the various noise parameters.

Finally, the simulation does not incorporate any of the non-linear phenomena that significantly affect real data. In section 6.1, we showed that a more sophisticated non-linear model should be adopted for simulating the actuator behaviour. Other phenomena not mentioned in the paper should also be simulated: calibration inaccuracies, harmonics, measuring device failures, limit cycle oscillations, ...

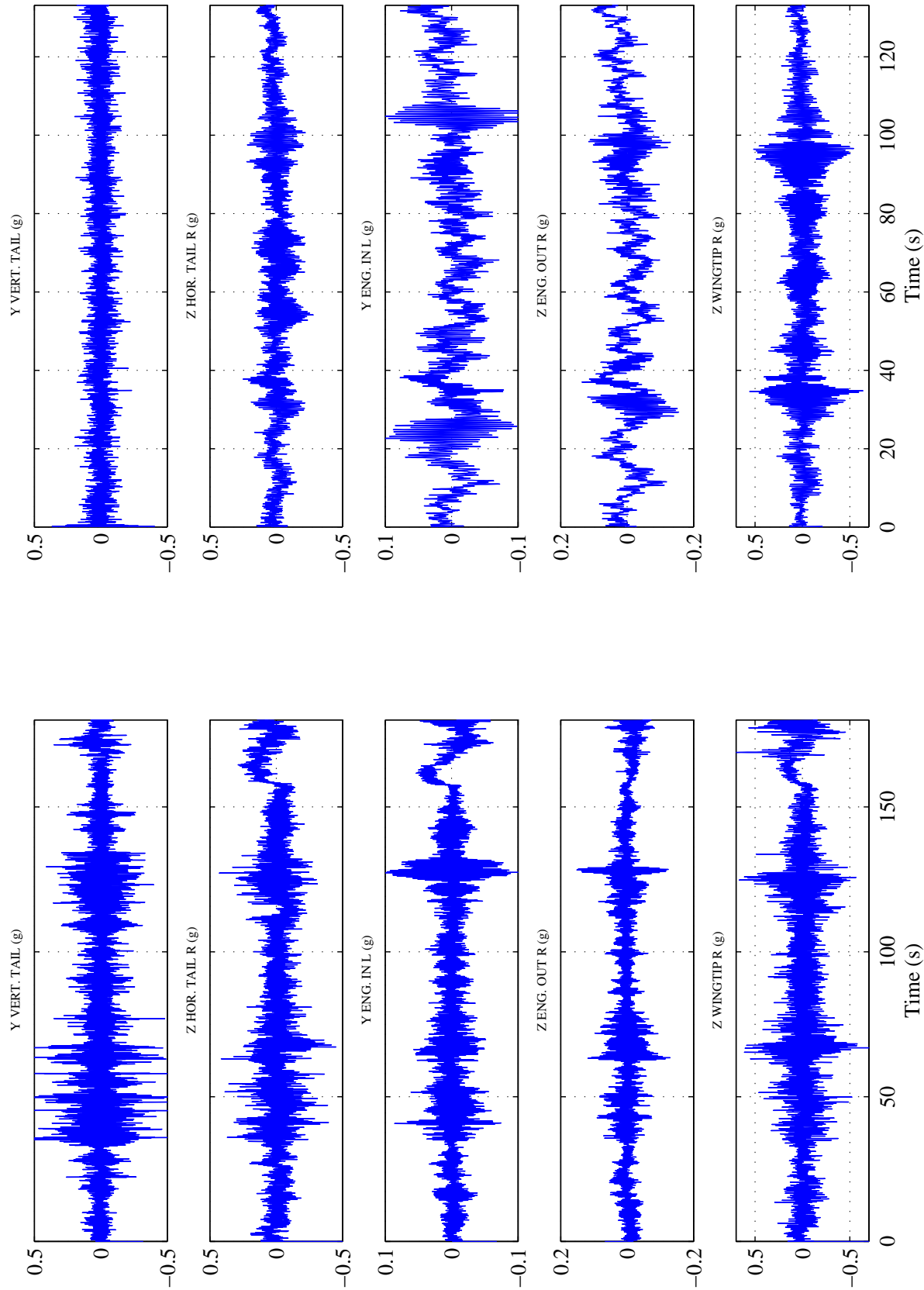


Figure 10: Comparison of real and simulated data for a sine-sweep test (Simulated data are in the right column).

Aircraft Model : Youpi – Acceleration from 330 to 360 kts – Mach = 0.86 – Test : No Excitation

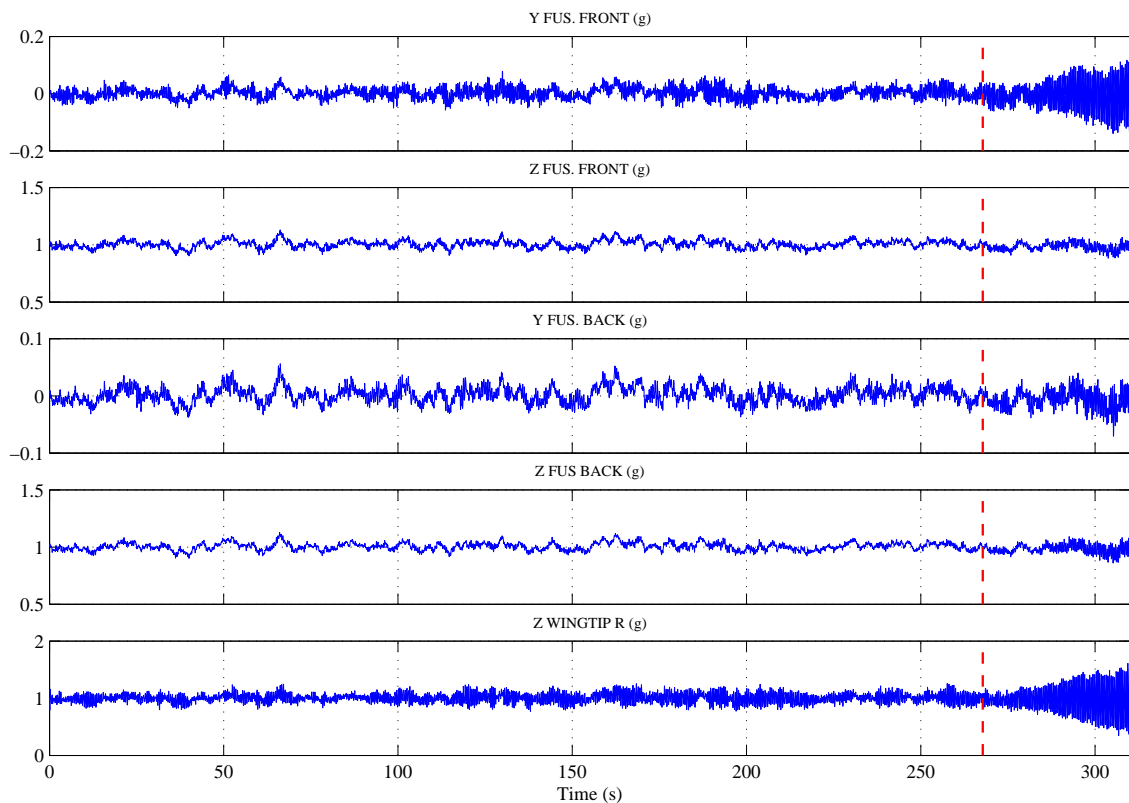


Figure 11: Transition phase without excitation

## Acknowledgements

It would not have been possible to carry out this study without the extensive collection of flight data maintained by Alain Buchardes and his acute analysis of the data. This simulation was entirely constructed on the aeroelastic model *Youpi* that was meticulously and lengthily concocted by Anne Pin-Belloc at Airbus. Finally, the authors would like to thank Anne Pin-Belloc, Cécile Daudet, Jean Roubertier at Airbus for their cordial cooperation during the FLITE 2 project.

## References

- [1] K. L. Roger. Airplane math modeling methods for active control design. In *AGARD-CP-228*, pages 4.1–4.11, 1977.
- [2] Germund Dahlquist and Åke Björck. *Numerical Methods*. Series in Automatic Computation. Prentice-hall, Inc., Englewood Cliffs, New Jersey, 1974.
- [3] Francis B. Hildebrand. *Introduction to Numerical Analysis*. Dover Publications, Inc., New York, 1987.
- [4] J.C. Butcher. *Numerical Methods for Ordinary Differential Equations*. Wiley, John & Sons, Incorporated, 2 edition, July 2003. ISBN: 0471967580.
- [5] Pierre Vacher. Mode alteration in the numerical integration of linear systems (version 1.0). Online Scientific Report TR 7/12645 DCSD, ONERA, Toulouse Center; 2, Avenue E. Belin, B.P. 4025, F-31055 TOULOUSE CEDEX 4, February 2008. <http://www.cert.fr/dcsd/idco/perso/Vacher>.

- [6] Bernard Etkin. *Dynamics of Atmospheric Flight*, chapter 13. John Wiley & Sons, Inc., June 1972.
- [7] Bernard Etkin. Turbulent wind and its effects on flight. *Journal of Aircraft*, 18(5):327–345, May 1981.
- [8] Jan Roskam. *Airplane Flight Dynamics and Automatic Flight Controls*, chapter 9. Roskam Aviation and Engineering Corporation, 2nd edition edition, 1979.
- [9] Alan V. Oppenheim and Ronald W. Schaffer. *Discrete-Time Signal Processing*. Signal Processing Series. Prentice Hall, Inc., Englewood Cliffs, New Jersey, 07632, 1989.
- [10] Peter D. Welch. The use of the fast fourier transform for the estimation of power spectra: a method based on time averaging over short modified periodograms. *IEEE Transactions on Audio Electroacoustics*, AU-15(2):70–73, June 1967.
- [11] Edwin Van Der Ouderaa, Johan Schoukens, and Jean Renneboog. Peak factor minimization of input and output signals of linear systems. *IEEE Transactions on Instrumentation and Measurement*, 17(2):207–212, June 1988.